Colloids and Surfaces A: Physicochemical and Engineering Aspects 691 (2024) 133852

Contents lists available at ScienceDirect

Colloids and Surfaces A: Physicochemical and Engineering Aspects

journal homepage: www.elsevier.com/locate/colsurfa

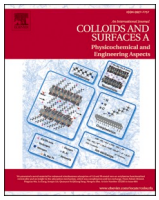

Honey-assisted synthesis and properties of silver nanoparticles in aqueous solution and inside supramolecular aggregates. The Cassyopea® effect

Carla Gasbarri *, Guido Angelini

Department of Pharmacy, University "G. d'Annunzio" of Chieti-Pescara via dei Vestini, Chieti 66100, Italy

HIGHLIGHTS

- Silver nanoparticles (NewAgNPs®) were made from honey into liposomes (Cassyopea®).
- Cassyopea® preserves the properties of NewAgNPs® acting as reactor and carrier.
- NewAgNPs® in solution and inside Cassyopea® were successfully tested against bacteria.

GRAPHICAL ABSTRACT

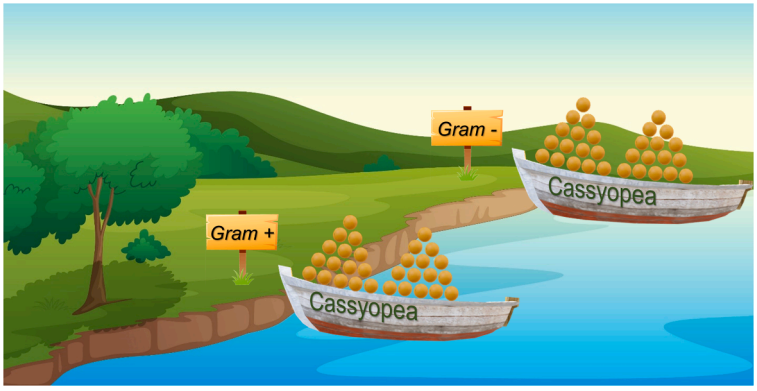

ARTICLE INFO

Keywords:
Sustainability
Liposomes
Silver nanoparticles
Honey
Antibacterial
Nanotechnology

ABSTRACT

In this work we introduce supramolecular aggregates named Cassyopea®, acronym of ***c**ombined **a**nd **s**ustainable **s**ynthesis **o**f **p**ayload-**e**nriched **a**ggregates* from the method used for their preparation. Herein, Cassyopea® were described as reactors and carriers for silver nanoparticles (AgNPs) obtained from honey according to eco-friendly conditions. Spherical, monodisperse, and negatively charged NewAgNPs®, acronym of *natural ecosustainable way* AgNPs, having a mean size of 30 nm and high stability over time were prepared in aqueous solution. The successful synthesis of NewAgNPs® inside Cassyopea® was demonstrated by UV–vis spectroscopy, emission scanning electron microscopy (FE-SEM) and energy-dispersive X-ray (EDX) analysis. The protective effect of Cassyopea® on NewAgNPs® against the oxidation induced by H_2O_2 was kinetically determined in the Fenton-like reaction suggesting that the investigated nanoparticles tend to be located in the aqueous core of the investigated aggregates. Furthermore, microbiological assays revealed the tendency of Cassyopea® to preserve the biological activity of NewAgNPs® against Gram-positive and Gram-negative bacteria. The preparation of silver nanoparticles directly into supramolecular aggregates instead of their loading in preformed state is unprecedented, and the data reported for NewAgNPs® and Cassyopea® highlight promising applications in nanotechnology.

* Corresponding author.
E-mail address: carla.gasbarri@unich.it (C. Gasbarri).

https://doi.org/10.1016/j.colsurfa.2024.133852
Received 5 February 2024; Received in revised form 13 March 2024; Accepted 29 March 2024
Available online 30 March 2024

1. Introduction

Liposomes are spherical supramolecular aggregates from phospholipids in aqueous solution extensively investigated as model membranes and drug delivery systems due to their composition and ability to incorporate hydrophilic compounds into the aqueous core and hydrophobic compounds into the lipid bilayer as guest [1–3]. Interestingly, the structural and chemical properties of these aggregates, including size, membrane integrity, microviscosity, and encapsulation efficacy may depend on the method of preparation, the presence and nature of guest molecules, and the charge of the lipid headgroup [4–11]. In most cases, liposomes revealed therapeutic effect for themselves, so that they could not be considered only as carriers for drug delivery [12,13].

Combination of supramolecular aggregates and metal nanoparticles was recently reported for theragnostic applications [14] and efficient biological activity was demonstrated in the case of liposomes loading silver nanoparticles [15–18]. Among the noble metals, silver nanoparticles (AgNPs) offer unique properties by which their range of application includes textile engineering, wound dressings, cosmetics, electronics, disinfectants, optical nanostructures, nanofluids and supramolecular nanomaterials [19,20]. For their well-known versatility AgNPs can be found into cosmetics, healthcare, everyday products and in the last years their commercial production has been continuously growing due to their efficacy mainly as antimicrobial, antiviral, and fungicidal agents. Moreover, the biodistribution and toxicity were also deeply investigated [21,22].

Generally, the use of AgNPs depends on their size and shape and may be optimized by adding stabilizers during the synthesis to prevent the self-aggregation [23–27]. Different methods of preparation based on chemical, physical and biological strategies can be adopted, including photochemical process and laser ablation. However, the most common synthesis of AgNPs consists of the chemical reduction of silver ions, which occurs in the presence of a reducing agent such as sodium borohydride, sodium citrate or ascorbate, *N*,*N*-dimethylformamide, and formamide. The most used stabilizers are polyvinylpyrrolidone and citrate added to the metal salt solution during the reaction to coat the silver surface and avoid the nanoparticle aggregation. The main limits of the chemical reduction consist of the processing of the organic reagents after the synthesis of the AgNPs and the interactions between the capping agents and the electrolytes dissolved in aqueous solution [28,29].

Recently, a series of eco-friendly approaches was proposed to generate spherical and monodisperse silver nanoparticles starting from plant extracts, microorganisms, or organic waste [30–34] by which natural compounds promote the reduction of Ag^+ ions into metallic Ag^0 and avoid the addiction of stabilizers and coating agents [35,36].

The honey-mediated synthesis of silver nanoparticles represents one of the most green and fast method to obtain AgNPs with controlled size and efficient biological activity [37–39]. Interestingly, supramolecular formulations based on the encapsulation of honey and derivatives demonstrated excellent properties [40,41] nevertheless these systems are still marginally reported. To the best of our knowledge the honey-assisted synthesis of AgNPs directly into liposomes was not previously proposed and the association of liposomes, honey and silver in the investigated conditions is unprecedented.

The aim of our work has been the synthesis of silver nanoparticles from honey according to a *natural ecosustainable way* (NewAgNPs®) in aqueous solution and inside biocompatible liposomes named Cassyopea®, acronym of ***c**ombined **a**nd **s**ustainable **sy**nthesis **o**f **p**ayload-enriched **a**ggregates* from the method used for their preparation.

Cassyopea® may preserve the properties of the investigated nanoparticles, facilitate their administration, and enhance their applications acting both as reactor and carrier. The easy and not-expensive experimental conditions, the high versatility and reproducibility represent some of the most remarkable advantages of the proposed aggregates.

Different techniques as UV–vis spectroscopy, dynamic light scattering, zeta potential, field emission scanning electron microscopy (FE-SEM), energy-dispersive X-ray spectroscopy (EDX) were employed to characterize the NewAgNPs® and the Cassyopea® samples. Moreover, the Fenton-like reaction of the dissolution of metallic silver induced by hydrogen peroxide and the microbiological assays on selected Gram-positive and Gram-negative bacteria were performed to demonstrate the effect of Cassyopea® on the stability and the antibacterial activity of NewAgNPs®. To the best of our knowledge the direct synthesis of silver nanoparticles from honey inside the supramolecular carrier instead of their loading as preformed AgNPs is reported for the first time and could contribute to the field of supramolecular chemistry combined with nanotechnology.

2. Experimental section

2.1. Materials

Silver nitrate ($AgNO_3$) 0.01 M purity 99.5% was purchased from Honeywell-Fluka; 1-palmitoyl-2-oleoyl-phosphatidylcholine (POPC) purity > 99% was purchased from Sigma-Aldrich. Italian *Acacia* honey was purchased directly from the beekeeper and used without further purification; hydrogen peroxide (H_2O_2) 30% was purchased from Sigma-Aldrich. All samples were diluted with Milli-Q water.

2.2. Preparation of NewAgNPs® and Cassyopea® samples

The synthesis of silver nanoparticles was performed by gradually mixing an aliquot of $AgNO_3$ 0.01 M to an aliquot of 1% *Acacia* honey aqueous solution at basic pH under stirring at room temperature until the color of the solution turns into the intense yellow. The silver concentration in the NewAgNPs® sample diluted to neutral pH corresponds to 2.5×10^{-5} M.

The Cassyopea® aggregates used in this work consists of POPC large unilamellar vesicles prepared by hydration of the phospholipidic film followed by extrusion according to the method previously described [8]. In brief, an aliquot of a 13 mM POPC organic solution was placed in a flask and the organic solvent was removed by evaporation under vacuum to obtain a dry film used as reaction medium for the synthesis of the NewAgNPs® as described above. The silver nanoparticles were generated inside liposomes and not loaded in preformed state. The silver and POPC concentrations in the Cassyopea® sample diluted to neutral pH corresponds to 2.5×10^{-5} M and 1.6×10^{-4} M, respectively.

2.3. Instruments

The spectroscopic analysis was performed by transferring 2 mL of the NewAgNPs® and Cassyopea® aqueous solution in 1 cm light path quartz cuvettes. The UV–vis spectra were recorded at 25 ± 0.1 °C by using a spectrophotometer Jasco V-570 (Jasco corporation, Tokyo, Japan).

Dynamic light scattering analysis and zeta potential measurements were carried out at 25 ± 0.1 °C by transferring 2 mL of the NewAgNPs® and Cassyopea® aqueous solution in disposable 1 cm light path cells. The scattering data were extrapolated by using the Stokes–Einstein relationship for the calculation of the hydrodynamic radius with a Brookhaven (90PLUS BI-MAS) digital correlator at a scattering angle of 90°. The instrument was equipped with a 35 mW He–Ne laser at the wavelength of 660 nm. For the zeta potential data, the angle of 15° instead of 90° was employed.

2.4. Ion selective electrode (ISE) analysis

The formation of NewAgNPs® was determined by measuring the concentration of Ag^+ in the sample after the reduction to Ag^0 at room temperature according to the method previously described [42]. The reference solution of $AgNO_3$ 0.01 M was used to obtain the 10 mL calibration curve standard solutions in the range 5–500 ppm. The silver

selective electrode (XS Sensors filled with KNO_3 1 M, with silver pin for argentometric titration) was conditioned for 60 min in the reference solution before using. All measurements were performed at 25 ± 0.1 °C after conditioning the electrode for 10 minutes into each sample.

2.5. FE-SEM and EDX analysis

The NewAgNPs® and Cassyopea® aqueous solutions were centrifugated and redispersed in water. Several drops of the obtained samples were placed on aluminium stubs using self-adhesive carbon conductive tabs and dried. The microscopical analysis was carried out after 24 h by using field emission scanning electron microscopy (FE-SEM, Sigma Family, Zeiss) and energy-dispersive X-ray spectroscopy (EDX, Quantax, EDS, Bruker).

2.6. Oxidation by Fenton-like reaction

An aliquot of H_2O_2 3% stock solution was added under stirring to 1 cm light path quartz cuvettes containing 2 mL of the diluted sample. The decreasing of the surface plasmonic band was used as evidence of the oxidation of metallic Ag^0 to Ag^+ ions. The pseudo first-order kinetic rate constants (k_{obs}) were spectroscopically measured at 25 ± 0.1 °C by monitoring the decreasing of the absorption band at 406 for NewAgNPs® sample and at 413 nm for Cassyopea® sample as a function of time.

2.7. Microbiological assays

The minimum inhibitory concentration (MIC) of NewAgNPs® and Cassyopea® was determined by means of the broth microdilution, following the method described by EUCAST for *E. coli* ATCC 25922, *P. aeruginosa* ATCC 27853, *S.aureus* ATCC 29213, and *B. cereus* [43]. Briefly, serial two-fold dilutions of each stock solution were obtained using Mueller Hinton broth (MHB). The plates containing 50 µL of the investigated aqueous solutions were inoculated with 50 µL of the bacterial suspension (1.5×10^6 CFU mL^{-1}) and incubated at 35 ± 1 °C overnight. The invitro antibacterial activity was tested against ciprofloxacin as reference. For MIC determinations *P. aeruginosa* ATCC 27853, and *S.aureus* ATCC 29213, were used as controls. The minimum bactericidal concentration (MBC) was determined by plating 100 µL of the bacterial suspension at the concentration ≥ MIC on Mueller Hinton Agar medium (MHA). The plates were incubated at 35 ± 1 °C overnight.

3. Results

The synthesis of NewAgNPs® mediated by honey occurs through turning the colorless silver nitrate aqueous solution into intense yellow and by the appearance of the typical surface plasmonic band at 406 nm suggesting the presence of spherical and monodisperse silver nanoparticles. The UV–vis spectrum of the NewAgNPs® in aqueous solution is reported in Fig. 1.

Interestingly, the absence of a broad absorption band around 650 nm allows to exclude the formation and the coexistence of silver oxide in solution [44].

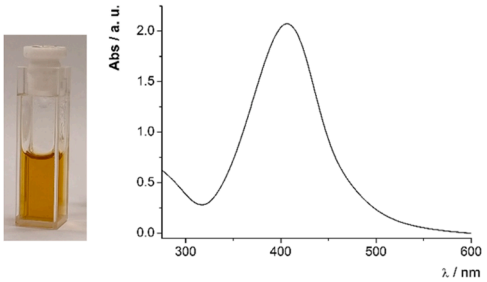

Fig. 1. UV–vis spectrum of the NewAgNPs® sample.

The concentration of silver ions in the NewAgNPs® sample was measured by Ion Selective Electrode (ISE) method. This technique is based on the linear correlation between the potential measured at the silver electrode and the Ag^+ concentration. It was found that the concentration of silver ion in the investigated solution is lower than the limit detection of the instrument suggesting that the reduction of Ag^+ into metallic Ag^0 was successfully completed in the experimental conditions.

The FE-SEM analysis and the EDX map are reported in Fig. 2. The FE-SEM images confirm the generation of silver nanoparticles highly homogeneous in size and nearly spherical in shape; the EDX analysis provides the optical absorption peak around 3 keV commonly observed for metallic silver [45].

The good level of monodispersion and homogeneity in the size and shape of the investigated nanoparticles were confirmed by the light scattering and surface charge analysis. The mean diameter, the polydispersity index, and the zeta potential of the NewAgNPs® are shown in Table 1.

The synthesis of the NewAgNPs® into the supramolecular system Cassyopea® successfully occurs as demonstrated by the turning of the colorless solution into intense clear yellow and by the appearance of the typical surface plasmonic band at 413 nm in the UV–vis spectrum as reported in Fig. 3.

As previously observed in the case of NewAgNPs® the broad band at 650 nm is missing in the Cassyopea® sample suggesting that no silver oxide is formed during the synthesis of the investigated nanoparticles inside the aggregates. The generation of homogeneous metallic silver nanoparticles into liposomes is also confirmed by the FE-SEM micrograph and the EDX map reported in Fig. 4.

The data from scattering and zeta potential analysis of Cassyopea® are shown in Table 2.

The results confirm the efficacy of the use of Cassyopea® as reactor for the synthesis of silver nanoparticles in the investigated conditions. To test the potential application of Cassyopea® as delivery system for the NewAgNPs® the kinetics of the oxidation of the metallic silver induced by H_2O_2 was determined according to the Fenton-like reaction [46,47]. The NewAgNPs® and Cassyopea® samples were exposed to the same amount of hydrogen peroxide at 25 ± 0.1 °C and neutral pH: the gradual decreasing of the absorbance at 406 and 413 nm, respectively, and the simultaneous turning from yellow into colorless for both solutions indicate the dissolution of the Ag^0 in agreement with a first order decay. The kinetic profiles obtained for the NewAgNPs® and Cassyopea® are reported in Fig. 5.

The pseudo first-order k_{obs} determined at 25 ± 0.1 °C for the Fenton-like reaction of the NewAgNPs® and Cassyopea® samples are reported in Table 3. The H_2O_2/Ag^0 ratio was kept constant and equal to 100/1 in all the experiments.

Finally, the minimum inhibitory concentration (MIC) and minimum bactericidal concentration (MBC) values of NewAgNPs® in aqueous solution and into Cassyopea® were obtained against four bacterial species having a well-known multidrug resistant phenotype: *Escherichia coli* and *Pseudomonas aeruginosa* were selected as Gram-negative bacteria, while *Staphylococcus aureus* and *Bacillus cereus* were selected as Gram-positive bacteria. The MIC and MBC values expressed in µg/mL obtained for the NewAgNPs® and Cassyopea® samples are reported in Table 4.

4. Discussion

Generally, narrow surface plasmonic band around 400 nm is observed for spherical silver nanoparticles in aqueous solution, while broadening or shifting to longer wavelength indicate the presence of aggregates. The intensity of the absorption band is strongly related to the yellowish color of the solution, while the amplitude depends on the shape and size so that blue or red shifting indicates the reduction or the increasing in the AgNPs dimensions, respectively. The determination of

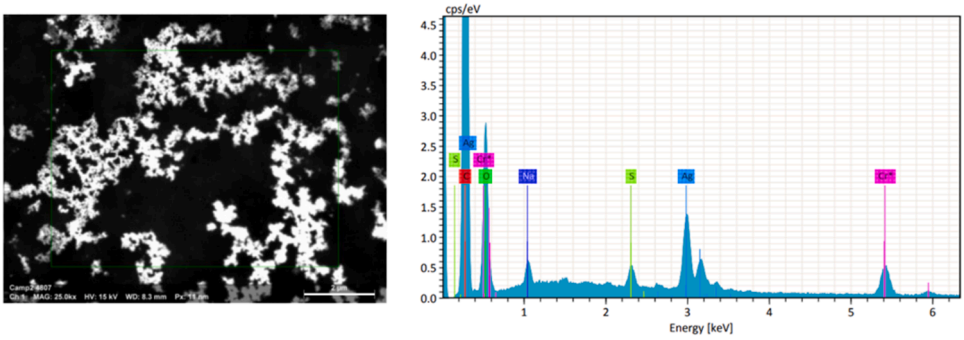

Fig. 2. FE-SEM images and EDX map of the NewAgNPs® sample. The scale bar is 2 μm.

Table 1
Size, polydispersity, and zeta potential values for the NewAgNPs® sample.

Mean size (nm)	Polydispersity	Zeta Potential (mV)
30.7 ± 0.3	0.36 ± 0.002	-35.8 ± 1.3

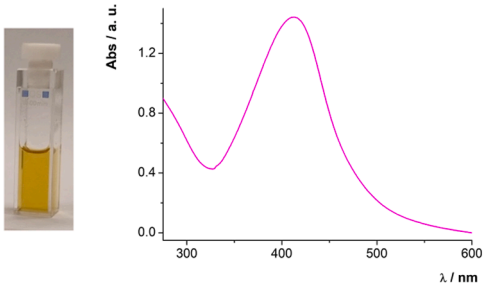

Fig. 3. UV–vis spectrum of the Cassyopea® sample.

the surface charge provides important information to predict the stability of the nanoparticles over time: large zeta potential value, independently on positive or negative sign, is measured in the case of high stability towards aggregation [48,49]. The FE-SEM analysis allows to detect size, morphology, and the presence of aggregates in the AgNPs sample, for this reason the data were often compared to the results from dynamic light scattering measurements by which the hydrodynamic diameter and particle distribution were obtained.

A homogeneous and monodisperse population of spherical NewAgNPs® in aqueous solution was obtained in the investigated conditions as demonstrated by the surface plasmonic band centered at 406 nm in the UV–vis spectrum (Fig. 1) and confirmed by the FE-SEM analysis (Fig. 2). In particular, the mean size and the polydispersity index (Table 1) agree with the range generally associated to strong antibacterial activity [50,51]. Interestingly, the negative zeta potential of −35 mV points out the tendency of the investigated nanoparticles to avoid aggregation phenomena. This behavior is confirmed by the fact that NewAgNPs® keep the average size for over 9 months by storing the

Table 2
Size, polydispersity, and zeta potential values for the Cassyopea® sample.

Mean size (nm)	Polydispersity	Zeta Potential (mV)
138.0 ± 2.2	0.19 ± 0.01	-69.5 ± 1.3

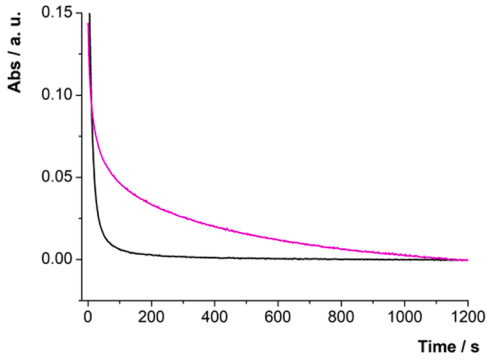

Fig. 5. Fenton-like kinetic profiles for NewAgNPs® (black line) and Cassyopea® (magenta line) samples at 25° C and neutral pH.

Table 3
Kinetic rate constant values (k_{obs}) for the NewAgNPs® and Cassyopea® samples at 25° C.

Sample	$k_{obs}/10^{-3}$ s^{-1}
NewAgNPs®	66.3 ± 0.2
Cassyopea®	3.08 ± 0.03

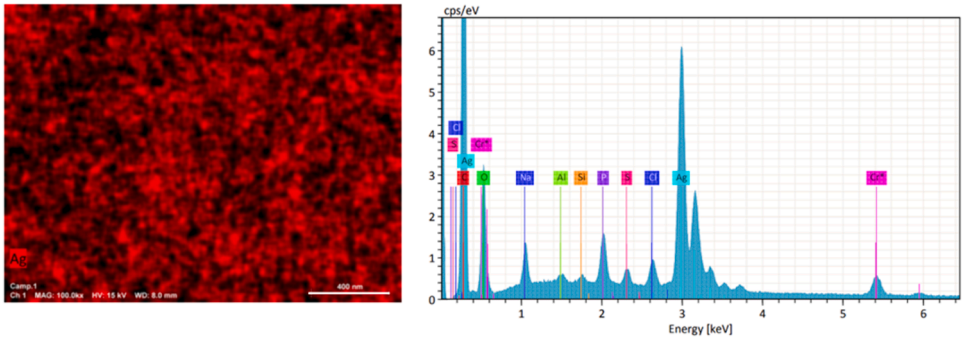

Fig. 4. FE-SEM image and EDX map of the Cassyopea® sample. In the micrograph Ag^0 is highlighted by using the red color. The scale bar is 400 nm.

Table 4
Minimum inhibitory concentration (MIC) and minimum bactericidal concentration (MBC) for the investigated samples. The values are expressed in μg/mL.

	NewAgNPs®		Cassyopea®	
Gram-negative	**MIC**	**MBC**	**MIC**	**MBC**
E. coli	5.4	5.4	9.1	9.1
P. aeruginosa	5.4	10.8	9.1	9.1
Gram-positive	**MIC**	**MBC**	**MIC**	**MBC**
S. aureus	5.4	> 10.8	4.55	> 9.1
B. cereus	5.4	> 10.8	> 9.1	Not detectable

sample at 4 °C.

The synthesis of silver nanoparticles directly inside liposomes as alternative to their loading in preformed state was performed according to a sustainable approach and spectroscopically and microscopically confirmed (Fig. 3 and Fig. 4). The sharp band centered at 413 nm in the Uv-vis spectrum of the Cassyopea® sample is compatible with the presence of the spherical and monodisperse NewAgNPs® indicating the successful role as Cassyopea® as reactor. The polydispersity index of 0.19 determined by scattering analysis as a measure of the statistic distribution of the aggregate size in the sample (Table 2) suggests that the formation of the investigated nanoparticles occurs inside liposomes highly monodisperse in aqueous solution. Moreover, the large negative surface charge value of −69.5 mV obtained for Cassyopea® by zeta potential analysis indicates that aggregation phenomena are hampered, and high stability can be expected. Similarly to NewAgNPs® the average dimension of Cassyopea® remains the same for over 9 months by storing the sample at 4 °C.

A stabilizing effect induced by Cassyopea® on NewAgNPs® can be pointed out by the kinetic profile and the k_{obs} determined in the Fenton-like reaction by which the rate of dissolution induced by hydrogen peroxide on the metallic silver was studied. The classical Fenton reaction consists of the oxidation process in which H_2O_2 reacts with ferrous ions to generate the highly bactericidal hydroxyl radicals and ferric ions. In the Fenton-like reaction transition metal ions are involved for the *in-situ* generation of reactive oxygen species. In the case of silver nanoparticles, the production of both hydroxyl radicals and antibacterial Ag^+ in the presence of hydrogen peroxide promotes a remarkable synergistic effect [52].

It was previously observed that the kinetic rate constant of the reaction (k_{obs}) is independent on the silver nanoparticles concentration but tends to increase linearly with the H_2O_2 concentration in the range 0.5–10 mM [46]. The data obtained for the investigated samples agree with the results previously described for capped AgNPs. In one of these studies, Ho *et al.* reported the kinetics of silver nanoparticles prepared by reduction of silver nitrate with sodium borohydride in the presence of sodium citrate as stabilizer [46]. In this case the value of the k_{obs} determined at 25 °C and neutral pH changes from 133 $\times 10^{-3}$ to 1.19 $\times 10^{-3}$ s^{-1} changing the H_2O_2/Ag^0 ratio from 200/1 to 2/1, respectively. In our experiments the H_2O_2/Ag^0 ratio was kept constant and equal to 100/1 and the k_{obs} determined for NewAgNPs® is very close to the k_{obs} extrapolated for the H_2O_2/Ag^0 ratio equal to 100/1 obtained by Ho and coworkers. In another work, Alkawareek *et al.* reported the kinetics of AgNPs prepared by reduction with $NaBH_4$ by using polyvinyl alcohol and polyallylamine hydrochloride as capping/stabilizing agents [47]. In this case, by considering the initial induction period of about 50 s in the dissolution of the Ag^0, the kinetics is completed within 180 s for the H_2O_2/Ag^0 ratio equal to 1/1. The reaction similarly occurs for the NewAgNPs® in the same conditions of temperature and pH but in the H_2O_2/Ag^0 ratio equal to 100/1. The higher concentration of H_2O_2 needed for the oxidation of NewAgNPs® to measure k_{obs} comparable to the capped AgNPs mentioned above can represent an indicator of the major stability of the investigated nanoparticles.

The NewAgNPs® synthesized into Cassyopea® show a slower oxidation rate and a k_{obs} value 21.5 times lower in comparison to the NewAgNPs® synthesized in aqueous solution (Table 3). Since the bilayer thickness of pure phosphatidylcholine liposomes was calculated around 4 nm the nanoparticle size should be lower than 4 nm to be located into the Cassyopea® bilayer [53]. Showing the average diameter of 30 nm (Table 1) NewAgNPs® are presumably located in the inner aqueous core of Cassyopea® so that hydrogen peroxide must permeate the bilayer to convert Ag^0 into Ag^+. Interestingly, at the end of the reaction the average size of Cassyopea® increases from 138 to 175 (± 0.7) nm suggesting that H_2O_2 permeation across the liposomal membrane occurs without altering the bilayer but enhancing the average size of the individual liposome [54,55].

This protective behavior seems to be reflected also in the biological activity of NewAgNPs® against the selected Gram-negative and Gram-positive bacteria listed in Table 4.

Generally, in the case of silver nanoparticles powerful antibacterial activity is associated with small size and small values of the minimum inhibitory concentration (MIC) and minimum bactericidal concentrations (MBC). The microbiological effect may be due either to release of Ag^+ from metallic silver or production of reactive oxygen species or direct interaction to specific macromolecules, as DNA, in the tested microorganism [56]. Moreover, inhibitory effects on the bacteria forming biofilm having resistance to antibiotic therapy were detected [57,58]. It was previously observed that the surface charge is also involved in the antimicrobial activity of silver nanoparticles: positively charged AgNPs possess the highest bactericidal properties, while the neutral AgNPs show the intermedia effect. The negatively charged AgNPs were associated with the lower activities [59].

Both NewAgNPs® and Cassyopea® samples show antibacterial activities against the selected Gram-negative and Gram-positive bacteria. In particular, MIC data of 5.4 for NewAgNPs® and 9.1 μg/mL for Cassyopea® were found against *E. coli*, *P. aeruginosa* and *B. cereus*. Interestingly, in the case of *S. aureus* a lower MIC (4.55 μg/mL) for Cassyopea® was obtained in comparison to NewAgNPs® (5.4 μg/mL), and in the case of *P. aeruginosa* a lower MBC (9.1 μg/mL) for Cassyopea® was measured in comparison to NewAgNPs® (10.8 μg/mL). Furthermore, the MBC/MIC ratio ≤ 2 indicates bactericidal properties of the NewAgNPs® in aqueous solution and inside Cassyopea®. These results agree with the data previously reported for commercial and naturally synthesized silver nanoparticles [60–63]. In the case of commercial AgNPs, less efficacy in comparison to NewAgNPs® was observed against *S. aureus*: the concentration of 0.625 mg/mL for the bactericidal activity of AgNPs having an average size of 5 nm and the concentration of 1.35 mg/mL for the bactericidal activity of AgNPs having an average size of 10 nm were determined.

It was previously demonstrated a size-dependent antibacterial activity by which kinetics and amount of Ag^+ release from metallic silver can be improved by reducing the nanoparticle dimensions. Moreover, the large surface area of small nanoparticles can easily interact with the bacteria cell altering its permeability [64]. The distribution of NewAgNPs® into the core of Cassyopea® liposomes was suggested by the oxidation data from the Fenton-like reaction. The delivery into Cassyopea® increases the overall size of the nanoparticles as a consequence of their inclusion but still preserve the biological effects as observed by the MIC and MBC values of the samples. It was also demonstrated that the control of dimension for the antibacterial use AgNPs is fundamental especially in the case of Gram-negative bacteria, in which there is an outer membrane external to the cell acting as a barrier. In the case of naturally synthesized AgNPs having diameter in the range 60–114 nm the MIC values of 563 μg/mL for *E. coli* and *P. aeruginosa* and of 1500 μg/mL for *S. aureus* were found, while in the case of naturally synthesized AgNPs having diameter in the range 20–22 nm the MIC value of 200 μg/mL and the MBC value of 400 μg/mL were determined for *P. aeruginosa* [65,66]. Our data suggest that the naturally synthesized NewAgNPs® possess remarkable antibacterial properties in comparison to larger and smaller nanoparticles and tend to conserve their notable biological effects carried into Cassyopea®.

5. Conclusions

Herein, we introduced the honey-mediated synthesis of NewAgNPs® performed in aqueous solution and inside Cassyopea® liposomes in the absence of reducing, coating, or stabilizing chemical reagents and without organic solvents according to the green approach. The combination of honey, silver nanoparticles and supramolecular aggregates is unprecedented as well as the formation of nanoparticles directly into liposomes. The generation of the investigated nanoparticles was spectroscopically, kinetically, and microbiologically tested. Cassyopea® demonstrated to act as reactor and carrier for NewAgNPs® both protecting the small, monodisperse, and spherical nanoparticles against the oxidation induced by hydrogen peroxide and preserving their bactericidal activities. In particular, MIC of 5.4 for NewAgNPs® and 9.1 μg/mL for Cassyopea® were found against *E. coli*, *P. aeruginosa* and *B. cereus*. Interestingly, in the case of *S. aureus* a lower MIC (4.55 μg/mL) for Cassyopea® was obtained in comparison to NewAgNPs® (5.4 μg/mL), while in the case of *P. aeruginosa* a lower MBC (9.1 μg/mL) for Cassyopea® in comparison to NewAgNPs® (10.8 μg/mL) was measured.

The high level of reproducibility, the sustainable conditions in which the synthesis of NewAgNPs® takes place, their remarkable stability, and the wide versatility of Cassyopea® open the door toward a wide range of applications in biological, physical, chemical, and technological fields.

CRediT authorship contribution statement

Carla Gasbarri: Writing – original draft, Resources, Methodology, Investigation, Conceptualization. **Guido Angelini:** Methodology, Investigation, Formal analysis, Data curation.

Declaration of Competing Interest

The authors declare that they have no known competing financial interests or personal relationships that could have appeared to influence the work reported in this paper.

Data availability

Data will be made available on request.

Acknowledgments

This work was supported by University “G. d’Annunzio” of Chieti-Pescara (FAR 2020). The authors thank the Italian Beekeepers Federation - Federazione Apicoltori Italiani (FAI) for the kind consultation. The authors also thank Prof. Clementina Cocuzza, Prof. Rosario Musumeci and Dr Federica Perdoni (School of Medicine and Surgery, University of Milano-Bicocca, Italy) for the microbiological analysis; Dr Laura Petetta (School of Science and Technology, Chemistry Division, University of Camerino, Italy) for SEM-EDX imaging.

Images for graphical abstract were taken for free from https://www.it.vecteezy.com.

Appendix A. Supporting information

Supplementary data associated with this article can be found in the online version at doi:10.1016/j.colsurfa.2024.133852.

References

[1] A.D. Bangham, R.W. Horne, Negative staining of phospholipids and their structural modification by surface-active agents as observed in the electron microscope, J. Mol. Biol. 8 (1964) 660–668, https://doi.org/10.1016/s0022-2836(64)80115-7.
[2] Y. Pierre, Gregory Gregoriadis: introducing liposomes to drug delivery, J. Drug Target 16 (2008) 518–519, https://doi.org/10.1080/10611860802228376.
[3] L. Sercombe, T. Veerati, F. Moheimani, S.Y. Wu, A.K. Sood, S. Hua, Advances and challenges of liposome assisted drug delivery, Front. Pharmacol. 6 (2015) 286, https://doi.org/10.3389/fphar.2015.00286.
C. Gasbarri, G. Angelini, A. Fontana, P. De Maria, G. Siani, I. Giannicchi, A. Della Cort, Kinetics of demetallation of a zinc–salophen complex into liposomes, Biochim. Biophys. Acta 1818 (2012) 747–752, https://doi.org/10.1016/j.bbamem.2011.10.014.
[5] O.G. Mouritsen, Lipids, curvature, and nanomedicine, Eur. J. Lipid Sci. Technol. 113 (2011) 1174–1187, https://doi.org/10.1002/ejlt.201100050.
[6] A. Gonzalez Gomez, S. Syed, K. Marshall, Z. Hosseinidoust, Liposomal nanovesicles for efficient encapsulation of staphylococcal antibiotics, ACS Omega 4 (2019) 10866–10876, https://doi.org/10.1021/acsomega.9b00825.
[7] M. Di Muzio, R. Millan-Solsona, A. Dols-Perez, J.H. Borrell, L. Fumagalli, G. Gomila, Dielectric properties and lamellarity of single liposomes measured by in-liquid scanning dielectric microscopy, J. Nanobiotechnol. 19 (2021) 167, https://doi.org/10.1186/s12951-021-00912-6.
[8] C. Gasbarri, G. Angelini, Spectroscopic investigation of fluorinated phenols as pH sensitive probes in mixed liposomal systems, RSC Adv. 4 (2014) 17840–17845, https://doi.org/10.1039/c4ra01507j.
[9] G. Angelini, C. Campestre, S. Boncompagni, C. Gasbarri, Liposomes entrapping β-cyclodextrin/ibuprofen inclusion complex: role of the host and the guest on the bilayer integrity and microviscosity, Chem. Phys. Lipids 209 (2017) 61–65, https://doi.org/10.1016/j.chemphyslip.2017.09.004.
[10] A. Yavlovich, A. Singh, S. Tarasov, J. Capala, R. Blumenthal, A. Puri, Design of liposomes containing photopolymerizable phospholipids for triggered release of contents, J. Therm. Anal. Calorim. 98 (2009) 97–104, https://doi.org/10.1007/s10973-009-0228-8.
[11] P. De Maria, A. Fontana, G. Siani, E. D’Aurizio, G. Cerichelli, M. Chiarini, G. Angelini, C. Gasbarri, Synthesis and aggregation behaviour of a new sultaine surfactant, Colloids Surf., B 87 (2011) 73–78, https://doi.org/10.1016/j.colsurfb.2011.05.003.
[12] P. Liu, G. Chen, J. Zhang, A review of liposomes as drug delivery system: current status of approved products, regolatoty environments and future prospectives, Molecules 27 (2022) 1372, https://doi.org/10.3390/molecules27041372.
[13] L. Van der Koog, T.B. Gandek, A. Nagelkerke, Liposomes and extracellular vesicles as drug delivery systems: a comparison of composition, pharmacokinetics, and functionalization, Adv. Heal. Mater. 11 (2022) 2100639, https://doi.org/10.1002/adhm.202100639.
[14] M. Musielak, J. Potoczny, A. Bos-Liedke, M. Kozak, The combination of liposomes and metallic nanoparticles as multifunctional nanostructures in the therapy and medical imaging-a review, Int. J. Mol. Sci. 22 (2021) 6229, https://doi.org/10.3390/ijms22126229.
[15] J.T. Espinoza, R.Schimandeiro Novak, C. Gonçalves Magalhães, J.Manfron Budel, B. Justus, M.Marques Gonçalves, P.Mathias D.öll Boscardin, P.V. Farago, J. de Fátima Padiha De Paula, Preparation and characterization of liposomes loaded with silver nanoparticles obtained by green synthesis, Braz. J. Pharm. Sci. 56 (2020) e18601, https://doi.org/10.1590/s2175-97902020000118601.
[16] P. Jayachandran, S. Ilango, V. Suseela, R. Nirmaladevi, M.Rafi Shaik, M. Khan, M. Khan, B. Shaik, Green synthesized silver nanoparticle-loaded liposome-based nanoarchitectonics for cancer management: in vitro drug release analysis, Biomedicines 11 (2023) 217, https://doi.org/10.3390/biomedicines11010217.
[17] A. Yusuf, A. Brophy, B. Gorey, A. Casey, Liposomal encapsulation of silver nanoparticles enhances cytotoxicity and causes induction of reactive oxygen species- independent apoptosis, J. Appl. Toxicol. 38 (2018) 616–627, https://doi.org/10.1002/jat.3566.
[18] A. Yusufa, A. Caseya, Evaluation of silver nanoparticle encapsulation in DPPC-based liposome by different methods for enhanced cytotoxicity, Int. J. Polym. Mater. Polym. Biomater. (2019) 860–871, https://doi.org/10.1080/00914037.2019.1626390.
[19] S.H. Lee, B.H. Jun, Silver nanoparticles: synthesis and application for nanomedicine, Int. J. Mol. Sci. 20 (2019) 865, https://doi.org/10.3390/ijms20040865.
[20] C. Gasbarri, G. Angelini, An overview on the role of cyclodextrins in the synthesis of silver nanoparticles by chemical reduction, Arkivoc iii (2022) 112–132, https://doi.org/10.24820/ark.5550190.p011.797.
[21] Z. Ferdous, A. Nemmar, Health impact of silver nanoparticles: a review of the biodistribution and toxicity following various routes of exposure, Int. J. Mol. Sci. 21 (2020) 2375, https://doi.org/10.3390/ijms21072375.
[22] Li Xu, Y.Y. Wang, J. Huang, C.Y. Chen, Z.X. Wang, H. Xie, Silver nanoparticles: synthesis, medical applications, and biosafety, Theranostics 10 (2020) 8996–9031, https://doi.org/10.7150/thno.45413.
[23] D.H. Kim, J.C. Park, G.E. Jeon, C.S. Kim, J.H. Seo, Effect of the size and shape of silver nanoparticles on bacterial growth and metabolism by monitoring optical density and fluorescence intensity, Biotechnol. Bioprocess Eng. 22 (2017) 210–217, https://doi.org/10.1007/s12257-016-0641-3.
[24] L. Wei, J. Lu, H. Xu, A. Patel, Z.-S. Chen, G. Chen, Silver nanoparticles: synthesis, properties, and therapeutic applications, Drug Discov. Today 20 (2015) 595–601, https://doi.org/10.1016/j.drudis.2014.11.014.
[25] Y. Xia, Z. Tang, Monodisperse inorganic supraparticles: formation mechanism, properties and applications, Chem. Comm. 48 (2012) 6320–6336, https://doi.org/10.1039/C2CC31354E.
[26] D. Amir, R.R. Nasaruddin, N.S. Engliman, S. Sulaiman, M.S. Mastuli, Effect of Stabilizers in the Synthesis of Silver Nanoparticles and Methylene Blue Oxidation, IOP Conf. Ser. Mater. Sci. Eng. 1192 (2021) 012031, https://doi.org/10.1088/1757-899X/1192/1/012031.

[27] G. Angelini, A. Pasc, C. Gasbarri, Curcumin in silver nanoparticles aqueous solution: Kinetics of keto-enol tautomerism and effects on AgNPs, Coll. Surf. A: Physicochem. Eng. Asp. 603 (2020) 125235, https://doi.org/10.1016/j.colsurfa.2020.125235.
[28] L. Gutierrez, C. Aubry, M. Cornejo, J.P. Croue, Citrate-coated silver nanoparticles interactions with effluent organic matter: influence of capping agent and solution conditions, Langmuir 31 (2015) 8865–8872, https://doi.org/10.1021/acs.langmuir.5b02067.
[29] S.A. Cumberland, J.R. Lead, Particle size distributions of silver nanoparticles at environmentally relevant conditions, J. Chromatogr. A 1216 (2009) 9099–9105, https://doi.org/10.1016/j.chroma.2009.07.021.
[30] T.C. Prathna, N. Chandrasekaran, A.M. Raichur, A. Mukherjee, Kinetic evolution studies of silver nanoparticles in a bio-based green synthesis process, Coll. Surf. A: Physicochem. Eng. Asp. 377 (2011) 212–216, https://doi.org/10.1016/j.colsurfa.2010.12.047.
[31] A. Gupta, S.M. Briffa, S. Swingler, H. Gibson, V. Kannappan, G. Adamus, M. Kowalczuk, C. Martin, I. Radecka, Synthesis of silver nanoparticles using curcumin-cyclodextrins loaded into bacterial cellulose-based hydrogels for wound dressing applications, Biomacromolecules 21 (2020) 1802–1811, https://doi.org/10.1021/acs.biomac.9b01724.
[32] G. Angelini, C. Gasbarri, Green synthesis and properties of silver nanoparticles in sulfobutylether-β-cyclodextrin aqueous solution, Colloids Surf. A: Physicochem. Eng. Asp. 633 (2022) 127924, https://doi.org/10.1016/j.colsurfa.2021.127924.
[33] A. Kumar, P.K. Vemula, P.M. Ajayan, G. John, Silver-nanoparticle-embedded antimicrobial paints based on vegetable oil, Nat. Mater. 7 (2008) 236–241, https://doi.org/10.1038/nmat2099.
[34] S. Ahmed, S. Ikram, Silver nanoparticles: one pot green synthesis using Terminalia arjuna extract for biological application, J. Nanosci. Nanotechnol. 6 (2015) 1000309, https://doi.org/10.4172/2157-7439.1000309.
[35] T.M. Abdelghany, A.M.H. Al-Rajhi, M.A. Al Abboud, M.M. Alawlaqi, A. Ganash Magdah, E.A.M. Helmy, A.S. Mabrouk, Recent advances in green synthesis of silver nanoparticles and their applications: about future directions. A review, BioNanoScience 8 (2018) 5–16, https://doi.org/10.1007/S12668-017-0413-3.
[36] P. Velusamy, J. Das, R. Pachaiappan, B. Vaseeharan, K. Pandian, Greener approach for synthesis of antibacterial silver nanoparticles using aqueous solution of neem gum (Azadirachta indica L.), Ind. Crops Prod. 66 (2015) 103–109, https://doi.org/10.1016/j.indcrop.2014.12.042.
[37] G.H. Matar, G. Akyüz, E. Kaymazlar, M. Andac, An investigation of green synthesis of silver nanoparticles using turkish honey against pathogenic bacterial strains, Bioint. Res. Appl. Chem. 13 (2023) 195, https://doi.org/10.33263/BRIAC132.195.
[38] D. Philip, Honey mediated green synthesis of silver nanoparticles, Spectrochim. Acta Part A 75 (2010) 1078–1081, https://doi.org/10.1016/j.saa.2009.12.058.
[39] G. Czernel, D. Bloch, A. Matwijczuk, J. Ciesla, M. Kedzierska-Matysek, M. Florek, M. Gagos, Biodirected synthesis of silver nanoparticles using aqueous honey solutions and evaluation of their antifungal activity against pathogenic Candida Spp, Int. J. Mol. Sci. 22 (2021) 7715, https://doi.org/10.3390/ijms22147715.
[40] N.A. Ramli, N. Ali, S. Hamzah, N.I. Yatim, Physicochemical characteristics of liposome encapsulation of stingless bees' propolis, Heliyon 7 (2021) e06649, https://doi.org/10.1016/j.heliyon.2021.e06649.
[41] N. Taïbi, R. Ameraoui, A. Kaced, M.A. Mustapha, A. Bouchama, A. Djafri, A. Taïbi, K. Mellahi, M. Hadjadj, S. Touati, F.Z. Badri, S. Djema, Y. Masmoudi, S. Belmiri, F. Khammar, Multifloral white honey outclasses manuka honey in methylglyoxal content: assessment of free and encapsulated methylglyoxal and anti-microbial peptides in liposomal formulation against toxigenic potential of Bacillus subtilis Subsp spizizenii strain, Food Funct. 13 (2022) 7591–7613, https://doi.org/10.1039/d2fo00566b.
[42] C. Gasbarri, F. Ruggieri, M. Foschi, A. Aceto, L. Scotti, G. Angelini, Simple determination of silver nanoparticles concentration as Ag^{+} by using ISE as potential alternative to ICP optical emission spectrometry, ChemistrySelect 4 (2019) 9501–9504, https://doi.org/10.1002/slct.201902336.
[43] European Committee for Antimicrobial Susceptibility Testing (EUCAST) of the European Society of Clinical Microbiology Infectious Diseases (ESCMID). Determination of minimum inhibitory concentrations (MICs) of antibacterial agents by broth dilution, Clin. Microbiol, Infect. 9 (2003) 1-7. https://doi.org/10.1046/j.1469-0691.2003.00790.x.
[44] O.A.Douglas Gallardo, R. Moiraghi, M.A. Macchione, J.A. Godoy, M.A. Pérez, E. A. Coronado, V.A. Macagno, Silver oxide particles/silver nanoparticles interconversion: susceptibility of forward/backward reactions to the chemical environment at room temperature, RSC Adv. 2 (2012) 2923–2929, https://doi.org/10.1039/C2RA01044E.
[45] M. Ider, K. Abderrafi, A. Eddahbi, S. Ouaskit, A. Kassiba, Silver metallic nanoparticles with surface plasmon resonance: synthesis and characterizations, J. Clust. Sci. 28 (2017) 1051–1069, https://doi.org/10.1007/s10876-016-1080-1.
[46] C.M. Ho, S.K.W. Yau, C.N. Lok, M.H. So, C.M. Che, Oxidative dissolution of silver nanoparticles by biologically relevant oxidants: a kinetic and mechanistic study, Chem. Asian J. 5 (2010) 285–293, https://doi.org/10.1002/asia.200900387.
[47] M.Y. Alkawareek, A. Bahlool, S.R. Abulateefeh, A.M. Alkilany, Synergistic antibacterial activity of silver nanoparticles and hydrogen peroxide, PLoS ONE 14 (2019) e0220575, https://doi.org/10.1371/journal.pone.0220575.
[48] K. Kolwas, A. Derkachova, M. Shopa, Size characteristics of surface plasmons and their manifestation in scattering properties of metal particles, J. Quant. Spectrosc. Radiat. Transf. 110 (2009) 1490–1501, https://doi.org/10.1016/j.jqsrt.2009.03.020.
[49] G. Angelini, L. Scotti, A. Aceto, C. Gasbarri, Silver nanoparticles as interactive media for the azobenzenes isomerization in aqueous solution: from linear to stretched kinetics, J. Mol. Liq. 284 (2019) 592–598, https://doi.org/10.1016/j.molliq.2019.04.048.
[50] Y. Dong, H. Zhu, Y. Shen, W. Zhang, L. Zhang, Antibacterial activity of silver nanoparticles of different particle size against Vibrio Natriegens, PlosOne 14 (9) (2019) e0222322, https://doi.org/10.1371/journal.pone.0222322.
[51] J.A. Lemire, J.J. Harrison, R.J. Turner, Antimicrobial activity of metals: mechanisms, molecular targets, and applications, Nat. Rev. Microbiol. 11 (2013) 371–384, https://doi.org/10.1038/nrmicro3028.
[52] E. Urnukhsaikhan, B. Bold, A. Gunbileg, N. Sukhbaatar, T. Mishig-Ochir, Antibacterial activity and characteristics of silver nanoparticles biosynthesized from Carduus crispus, Sci. Rep. 11 (2021) 21047, https://doi.org/10.1038/s41598-021-00520-2.
[53] P. Walde, S. Ichikawa, Enzymes inside lipid vesicles: preparation, reactivity, and applications, Biomol. Eng. 18 (2001) 143–177, https://doi.org/10.1016/S1389-0344(01)00088-0.
[54] V. Sitaramam, J.C. Mathai, N.M. Rao, L.H. Block, Hydrogen peroxide permeation across liposomal membranes: a novel method to assess structural flaws in liposomes, Mol. Cell. Biochem. 91 (1989) 91–97, https://doi.org/10.1007/BF00228083.
[55] N.P. Palmina, N.G. Bogdanova, N.N. Sazhina, N.N. Kasparov, V.I. Binyukov, I. G. Plashchina, A.S. Antipova, M.G. Semenova, The relationship between lipid peroxidation and microviscosity in phosphatidylcholine liposomes. The effects of a plant antioxidant and a protein, Biophysics 64 (2019) 551–559, https://doi.org/10.1134/s0006350919040146.
[56] F.A. Qais, A. Shafiq, H.M. Khan, F.M. Husain, R.A. Khan, B. Alenazi, A. Alsalme, I. Ahmad, Antibacterial effect of silver nanoparticles synthesized using Murraya koenigii (L.) against multidrug-resistant pathogens, Bioinorg. Chem. Appl. (2019) 4649506, https://doi.org/10.1155/2019/4649506.
[57] K. Kalishwaralal, S. Barath Mani Kanth, S.R.K. Pandian, V. Deepak, S. Gurunathan, Silver nanoparticles impede the biofilm formation by Pseudomonas aeruginosa and Staphylococcus epidermidis, Colloids Surf. B 79 (2010) 340–344, https://doi.org/10.1016/j.colsurfb.2010.04.014.
[58] X. Li, L. Sun, P. Zhang, Y. Wang, Novel approaches to combat medical device-associated biofilms, Coatings 11 (2021) 294, https://doi.org/10.3390/coatings11030294.
[59] A. Abbaszadegan, Y. Ghahramani, A. Gholami, B. Hemmateenejad, S. Dorostkar, M. Nbavizadeh, H. Sharghi, The effect of charge at the surface of silver nanoparticles on antimicrobial activity against Gram-positive and Gram-negative bacteria: a preliminary study, J. Nanomater. (2015) 1–8, https://doi.org/10.1155/2015/720654, 720654.
[60] E. Radzikowska-Büchner, W. Flieger, S. Pasieczna-Patkowska, W. Franus, R. Panek, I. Korona-Głowniak, K. Susniak, B. Rajtar, L. Swiatek, N. Zuk, A. Bogucka-Kocka, A. Makuch-Kocka, R. Maciejewski, J. Flieger, Antimicrobial and apoptotic efficacy of plant-mediated silver nanoparticles, Molecules 28 (2023) 5519, https://doi.org/10.3390/molecules28145519.
[61] P. Parvekar, J. Palaskar, S. Metgud, R. Maria, S. Dutta, The minimum inhibitory concentration (MIC) and minimal bactericidal concentration (MBC) of silver nanoparticles against Staphylococcus aureus, Biomater. Investig. Dent. 7 (1) (2020) 105–109, https://doi.org/10.1080/26415275.2020.1796674.
[62] Y.Y. Loo, Y. Rukayady, M.A.R. Nor-Khaizura, C.H. Kuan, B.W. Chieng, M. Nishibuchi, S. Radu, In vitro antimicrobial activity of green synthesized silver nanoparticles against selective Gram-negative foodborne pathogens, Front. Microbiol. 9 (2018) 1555, https://doi.org/10.3389/fmicb.2018.01555.
[63] M. Fernandes, N.G. Ballesteros, A. da Costa, R. Machado, A.C. Gomes, M. C. Rodríguez-Argüelles, Antimicrobial and anti-biofilm activity of silver nanoparticles biosynthesized with Cystoseira algae extracts, J. Biol. Inorg. Chem. 28 (2023) 439–450, https://doi.org/10.1007/s00775-023-01999-y.
[64] A.L. Mitchell, T.J. Silhavy, Envelope stress response: balancing damage repair and toxicity, Nat. Rev. Microbiol. 17 (2019) 417–428, https://doi.org/10.1038/s41579-019-0199-0.
[65] S. Ulagesan, T. Nam, Y. Choi, Biogenic preparation, and characterization of Pyropia yezoensis silver nanoparticles (P.y AgNPs) and their antibacterial activity against Pseudomonas aeruginosa, Bioprocess Biosyst. Eng. 44 (2021) 443–452, https://doi.org/10.1007/s00449-020-02454-x.
[66] G.A. Martínez-Castañón, N. Niño-Martínez, F. Martínez-Gutierrez, J.R. Martínez-Mendoza, F. Ruiz, Synthesis, and antibacterial activity of silver nanoparticles with different sizes, J. Nanopart. Res. 10 (2008) 1343–1348, https://doi.org/10.1007/s11051-008-9428-6.